doi:10.14311/ppt.2017.2.112
*Plasma Physics and Technology* **4**(2):112–115, 2017


# ADVANCED APPROACH FOR RADIATION TRANSPORT DESCRIPTION IN 3D COLLISIONAL-RADIATIVE MODELS

D. Kalanov[a], Yu. B. Golubovskii[a], D. Uhrlandt[b], S. Gortschakow[b,*]

[a] *Saint Petersburg State University, 7/9 Universitetskaya nab., 199034 St. Petersburg, Russia*

[b] *Leibniz Institute for Plasma Science and Technology (INP Greifswald), Felix-Hausdorff-Str. 2, 17489 Greifswald, Germany*

[*] sergey.gortschakow@inp-greifswald.de

**Abstract.** The description of radiation transport phenomena in the frames of collisional-radiative models requires the solution of Holstein-Biberman equation. An advanced solutuion method for 3D plasma obejcts is proposed. The method is applicable for various line contours in a wide range of absorption coefficients. Developed approach is based on discretization of the arbitrary plasma volume on a Cartesian voxel grid. Transport of photons between the cells is computed using the ray traversal algorithm by Amanatides [1]. Solution of the particle balance equations with computed in advance radiative transfer matrix is demonstrated for various typical arc shapes, like e.g. free-burning arc and cylindric arc. Results are compared with corresponding calculations using previously developed approaches. As the method is suited for finite geometries and allows for a strict solution of the radiation transport equation, applicability ranges of previous approximations can be specified.

**Keywords:** radiation transport, resonance radiation, plasma modelling, arcs.

## 1. Introduction

Trapping of line radiation is a fundamental problem of gas discharge physics. Over the years a Holstein's approximation of effective transition probability [2] was used to evaluate the influence of radiation trapping. This approximation describes the photon escape taking absorption into account rather roughly and fails to describe the correct spatial redistribution of resonance atoms. The description of radiation transport phenomena in the frames of collisional-radiative models requires the solution of Holstein-Biberman equation [3]. Various solution methods of this equation were proposed over the years (see, for example, [3, 4]). One of promising solution approaches is the matrix method [3]. A kernel of the integral operator is represented as a matrix, which can be successfully coupled with self-consistent plasma models [5, 6]. Despite the low computational cost and simple integration into plasma-chemical schemes, this method, as well as an another matrix approach [7], has certain limits.

The main drawback is related to the plasma domain geometry. Depending on the shape of a plasma source, a discretization scheme should be specified. In mentioned appoaches the scheme was chosen based on the source symmetry (plane-parallel, infinite and finite cylinder). An analytical conversion of the kernel to the convenient form was performed, where each type of symmetry had a unique kernel representation. Finite domains require extensive mathematical treatment. Furthermore, the case of an asymmetric domains was beyond the scope of the method. In addition, inhomogeneity of absorption spatial profile significantly complicated the derivation of suitable radiation transport matrix.

In present work an advanced matrix method is described. It provides a solution approach for the Holstein-Biberman equation on a uniform cartesian grid, which is universal for various 3D domains. The method allows for the strict integration over the frequency having spatial integrals fully discretized. Results of computations are compared to data obtained with previously developed methods and demonstrated for typical arc plasma domains.

## 2. Description of the method

### 2.1. Basic equations

The Holstein-Biberman equation for the case of stationary plasma reads

$$W(\vec{r}) = N(\vec{r}) \cdot A - \int\limits_V N(\vec{r}\,') \cdot A \cdot K(\vec{r}, \vec{r}\,')\mathrm{d}^3 r'. \quad (1)$$

Here $N(\vec{r})$ is the population of the excited level (density of excited atoms), $W(\vec{r})$ represents the excitation source, and $A$ is the spontaneous emisson probability. The kernel $K(\vec{r}, \vec{r}\,')$ describes the absorption in the point $\vec{r}$ of photons emitted in the point $\vec{r}\,'$:

$$K(\vec{r}, \vec{r}\,') = \frac{1}{4\pi} \int\limits_0^\infty \mathrm{d}\nu \frac{\varepsilon_\nu(\vec{r}\,')\kappa_\nu(\vec{r})}{|\vec{r} - \vec{r}\,'|^2} \exp\left( - \int\limits_{\vec{r}\,'}^{\vec{r}} \kappa_\nu(\xi)\mathrm{d}\xi \right). \quad (2)$$

Under the assumption of complete frequency redistribution the line profiles of emission and absorption

$\varepsilon_\nu$,$\kappa_\nu$ fulfil the criteria

$$\int_0^\infty \varepsilon_\nu \mathrm{d}\nu = 1, \qquad \kappa_\nu = \kappa_0 \frac{\varepsilon_\nu}{\varepsilon_0}.$$

Here $\varepsilon_0$ and $\kappa_0$ are the values in the line center.

For the sake of simplicity further derivation will be performed for the case of homogeneous absorption over the volume. Therefore, the kernel becomes the representation

$$K(\vec{r},\vec{r}\,') = \frac{1}{4\pi}\int_0^\infty \mathrm{d}\nu \frac{\varepsilon_\nu \kappa_\nu}{|\vec{r}-\vec{r}\,'|^2} \exp\left(-\kappa_\nu |\vec{r}-\vec{r}\,'|\right). \tag{3}$$

To make the problem discrete the integral operator in (1) will be replaced by a matrix dividing the entire volume into a number af small finite cells: $V = \sum_{i=1}^{M} \Delta V_i$, where $M$ is a number of cells. Parameters in plasma are assumed to be constant within the subvolume. The equation (1) then becomes

$$\begin{aligned} W(r_k) &= \sum_{i=1}^{M} N(r_i) a_{ik}, \\ a_{i,k} &= A \cdot \left( \delta_{i,k} - \int_{\Delta V_i} K(r_k, r')\mathrm{d}^3 r' \right). \end{aligned} \tag{4}$$

In order to calculate the integrals in (4) a certain discretization scheme has to be chosen.

## 2.2. Calculation of the matrix elements

In the present approach a universal discrete scheme based on an uniform cartesian 3D-grid (or "voxel grid") is used. An extension of the approach for the case of the non-uniform grids is also possible.

To calculate the distances between the points $\vec{r}$ and $\vec{r}\,'$, a fast voxel traversal algorithm by Amanatides and Woo [1] was implemented. This algorithm casts the ray from one voxel to another and counts all voxels that have been crossed. The distance between the points $\vec{r}$ and $|\vec{r}-\vec{r}\,'| = \rho$ can be associated with indices $i,k$ for each cell:

$$\rho_{i,k} = \Delta l \sqrt{(x_i-x_k)^2 + (y_i-y_k)^2 + (z_i-z_k)^2} \qquad i,k = 1..M. \tag{5}$$

Here $x, y, z$ denote integer voxel coordinates, $M$ is a total number of voxels, $\Delta l = \sqrt[3]{\Delta V}$ is a length of the voxel edge relative to the source volume. Considering the homogeneous absorption only the knowledge of $i$ and $k$ is necessary. In order to account for the inhomogeneity the coordinates of all crossed voxels should be used.

Introducing a dimensionless distance $\widetilde{\rho}_{i,k} = \rho_{i,k}/\Delta l$, the general form of matrix coefficient reads:

$$a_{i,k} = A \cdot \left( \delta_{i,k} - \Delta V \int_0^{\widetilde{\rho}_{i,k}} K(\widetilde{\rho})\mathrm{d}\widetilde{\rho} \right). \tag{6}$$

In the case of homogeneous absorption ($\kappa_\nu(r) = \kappa_\nu$) the integral in exponent (2) is reduced to $\kappa_\nu \rho_{i,k}$. The discretization of the kernel requires consideration of two different cases.

$i \neq k$: in this case $\rho \neq 0$ and (6) can be rewritten as

$$a_{i,k} = -A \cdot \frac{\Delta V}{4\pi} \int_0^\infty \frac{\varepsilon_\nu \kappa_\nu}{\rho_{i,k}^2} \exp\left(-\kappa_\nu \rho_{i,k}\right) \mathrm{d}\nu \tag{7}$$

For the case $i = k$: in $\rho = 0$ the integral has a singularity. It can be eliminated by the conversion to spherical coordinates considering $\rho_{i,i} \to \Delta r$:

$$\begin{aligned} a_{i,i} &= A \cdot \left[ 1 - \frac{1}{4\pi} \int_0^\infty \left( 4\pi \int_0^{\rho_{i,i}} \frac{\varepsilon_\nu \kappa_\nu}{\rho'^2} e^{-\kappa_\nu \rho'} \rho'^2 \mathrm{d}\rho' \right) \mathrm{d}\nu \right] = \\ &= A \cdot \left[ 1 - \int_0^\infty \left( \int_0^{\Delta r} \varepsilon_\nu \kappa_\nu e^{-\kappa_\nu r} \mathrm{d}r \right) \mathrm{d}\nu \right]; \quad \Delta r = \sqrt[3]{\frac{3\Delta V}{4\pi}}. \end{aligned} \tag{8}$$

Finally, the matrix coefficients in the case of homogeneous absorption ($\kappa_\nu(r) = \kappa_\nu$) are given by

$$a_{i,k} = A \cdot \begin{cases} -\frac{\Delta V}{4\pi} \int_0^\infty \frac{\varepsilon_\nu \kappa_\nu}{\xi_{i,k}^2} e^{-\kappa_\nu \Delta l} \mathrm{d}\nu, & i \neq k; \\ 1 - \int_0^\infty \left( \int_0^{\Delta r} \varepsilon_\nu \kappa_\nu e^{-\kappa_\nu r} \mathrm{d}r \right) \mathrm{d}\nu, & i = k. \end{cases} \tag{9}$$

Considering the case of the Lorentzian line shape and spatially homogeneous absorption the simplified expressions for matrix coefficients can be derived to speed up the computation. The kernel can be rewritten in following form

$$K(\vec{r},\vec{r}\,') = -\frac{1}{4\pi|\vec{r}-\vec{r}\,'|^2} \frac{\mathrm{d}T}{\mathrm{d}\rho}\Big|_{\rho=|\vec{r}-\vec{r}\,'|}, \tag{10}$$

where $T(\rho)$ is a Biberman's transmission factor:

$$T(\rho) = \int_0^\infty \varepsilon_\nu e^{-\kappa_\nu \rho} \mathrm{d}\nu = e^{-\frac{\kappa_0 \rho}{2}} I_0\left(\frac{\kappa_0 \rho}{2}\right). \tag{11}$$

Here $I_{\alpha=0,1,2...}$ denotes the modified Bessel function of the first kind. Then, the expression for the kernel reads

$$K(\rho) = \frac{1}{4\pi\rho^2} \cdot \frac{\kappa_0}{2} e^{-\frac{\kappa_0 \rho}{2}} \left[ I_0\left(\frac{\kappa_0 \rho}{2}\right) - I_1\left(\frac{\kappa_0 \rho}{2}\right) \right]. \tag{12}$$

Substituting of Eq.(12) into Eq. (6) gives

$$a_{i,k} = A \cdot \begin{cases} -\frac{\kappa_0 \Delta V}{8\pi\rho_{i,k}^2} e^{-\frac{\kappa_0 \rho_{i,k}}{2}} \left[ I_0\left(\frac{\kappa_0 \rho_{i,k}}{2}\right) - I_1\left(\frac{\kappa_0 \rho_{i,k}}{2}\right) \right], \\ e^{-\frac{\kappa_0 \Delta r}{2}} I_0\left(\frac{\kappa_0 \Delta r}{2}\right), \quad i = k. \end{cases} \tag{13}$$

The benchmark tests show that the computational time for elements decreases up to a factor of five comparing to numerical integration over the line contour.

### 2.3. Solution algorithm

A domain with a volume $V$ is discretized on a uniform cartezian grid using voxelizer code [8]. Characteristic linear size of the voxelized mesh is determined by the maximum number of voxels along the $x$-dimension $n_{\mathrm{dim}}$.

The matrix coefficients are computed in two steps: calculation of the distances traveled by photons $\rho_{i,k}$ and integration of the kernel 2) for each pair of voxels. In order to optimize the calculation of distances, ray tracing algorithm [1] was modified for parallel computing using a graphical processing unit (GPU). Each thread of GPU can handle the operations only with scalars, therefore, the vectors with coordinates of each $(r, r')$-pair are prepared. The number of voxel pairs being simultaneously processed (the array chunk size) is determined by the size of the graphics card memory. Then, the chunk with computed distances is transferred to the CPU where the coefficients (9) are calculated and stored in a file. After the loop over all chunks the saved data are collected in the matrix which represents the coupling between all cells in plasma.

When the radiation transport matrix is ready, the system of linear equations representing the Holstein-Biberman equation can be solved for a given excitation source in the plasma domain. This equation system can be also easily included into a multicomponent collisional-radiative model, which considers the coupling with particle transport equations for other plasma species.

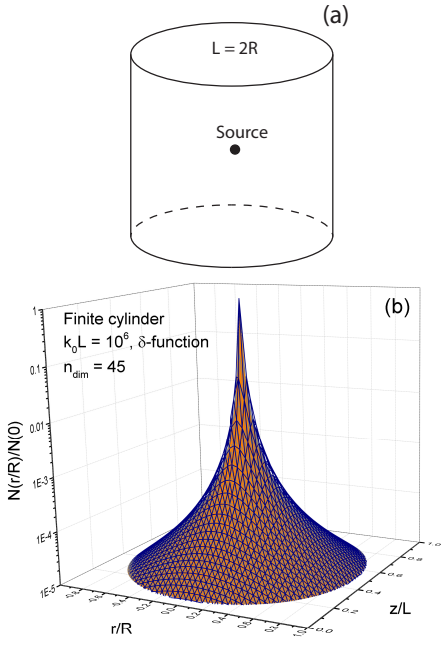


*Figure 1. (a) Scheme of the finite cylinder domain with a point excitation sourcein the center, (b) Spatial distribution of the density of resonance atoms in case of point source in the finite cylinder. Blue grid - ray tracing method, orange mesh - asymptotic matrix method.*

## 3. Results

To validate the approach a finite cylinder geometry of size $L = 2R = 1$ with a point excitation source located in the volume center was used. In previous publication [9] a similar problem was considered for the case of the high-opacity asymptotics for a Lorentzian line contour. The kernel of the radiation transport operator was integrated over cylindrical layer cells. The size of corresponding linear equation system was $n^2_{\mathrm{dim}}$. The same problem is solved by ray tracing method without the use of the asymptotics. The resulting linear equation system has the size of the order of $n^3_{\mathrm{dim}}$. Figure 1 demonstrates the schematic representation of the geometry as well as the solution of Eq. (4) using both methods for the case with an optical depth $\kappa_0 L = 10^6$. Linear mesh size for ray tracing method is $n_{\mathrm{dim}} = 45$. As it becomes obvious from Fig. 1 both approaches are in an excellent agreement. Similar results have been obtained for various values of the absorption coefficent as long as the later remained high.

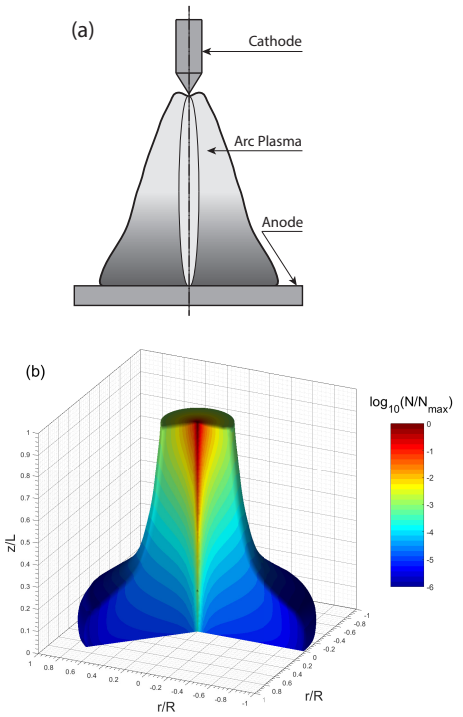


*Figure 2. (a) Schematic picture of a free-burning arc. (b) Normalized solution for the case of $n_{dim} = 41$, $k_0 L = 10^6$.*

The main advantage of the approach is the possibility to solve the radiation transport equation in an arbitrary 3D domain. As examples of non-trivial geometry a "bell"-like shape of a free-burning arc (welding arc) and two hemispherical electrodes (switching arc) were chosen. The size of the grid in both cases was $n_{\mathrm{dim}} = 41$ and the optical depth was set to $\kappa_0 L = 10^6$. The excitation source is approximated by a function $W(r) = 10^{-ar}$ along discharge axis.

The first example is illustrated by a Figure 2. Figure

2a present a schematic picture of the free-burning arc. Figure 2b demonstrates the solution of the Holstein-Biberman equation in a discretized 3D-domain.

A typical cylindrical circuit breaker geometry is presented in Figure 3a. The solution is demonstrated by Figure 3b. One could see the effects of radiation screening by electrodes. To include these effects one needs to exclude the coupling between unit volumes where photons cannot travel along the straight line. For this purpose, the check is performed whether the ray trace only allowed voxels or not.

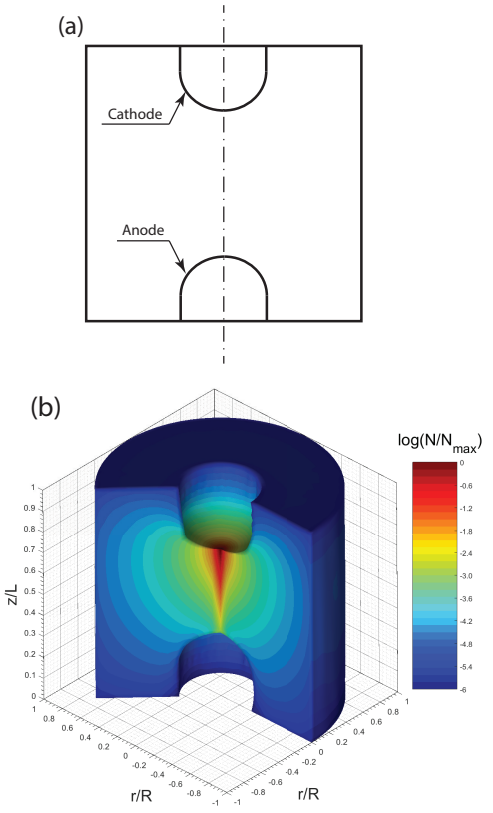


*Figure 3. (a) Schematic picture of a switching arc geometry. (b) Normalized solution for the case of* $n_{dim} = 41$, $k_0 L = 10^6$.

## 4. Conclusions

In the present work an advanced matrix method based on the ray tracing algorithm for the solution the Holstein-Biberman equation is proposed. The method is applicable for arbitrary 3D-domains discretized on a uniform Cartezian mesh. The transformation of the radiation transport operator was performed for the Lorentzian line shape and high opacity. The method can be extended for a wide range of absorption coefficients and is in general not dependent on the line shape. In the case of Lorentzian line shape and high opacity limit the matrix coefficients can be simplified to reduce the computation time.

The ability to solve the radiation transport equation in complex domains is illustrated by two examples: free-burning welding arc and cylindrical switching arc. The results demonstrate expected qualitative distribution of the radiation known from the experiments. Developed approach is compared with the previous matrix method for the case of a finite cylinder geometry with a point excitation source located in the center. The results of both approaches are in excellent agreement for the case of large absorption coefficients.

The radiation transport matrices computed with the ray tracing method can be successfully integrated into self-consisent multicomponent plasma models of various complexity.

## Acknowledgements

Authors gratefully acknowledge computational resources provided by Computer Center of Saint-Petersburg State University. The work of D.K. was also supported by German-Russian Interdisciplinary Science Center (G-RISC) P-2016b-17.

## References

[1] J. Amanatides and A. Woo. A Fast Voxel Traversal Algorithm for Ray Tracing. *Eurographics*, 87(3):3–10, 1987. doi:10.1.1.42.3443.

[2] T. Holstein. Imprisonment of resonance radiation in gases. *Physical Review*, 72(12):1212–1233, 1947. doi:10.1103/PhysRev.72.1212.

[3] Yu.B. Golubovskii, S. Gorchakov, and D. Uhrlandt. Transport mechanisms of metastable and resonance atoms in a gas discharge plasma. *Plasma Sources Science and Technology*, 22(2):32pp, 2013. doi:10.1088/0963-0252/22/2/023001.

[4] A.F. Molisch and B.P. Oehry. *Radiation trapping in atomic vapours*. Oxford University Press, 1998.

[5] Yu.B. Golubovskii and V.A. Maiorov. The influence of resonance radiation transport on the contraction of a glow discharge in argon. *Plasma Sources Science and Technology*, 24(2):25027, 2015. doi:10.1088/0963-0252/24/2/025027.

[6] Yu.B. Golubovskii, D. Kalanov, S. Gortschakow, M. Baeva, and D. Uhrlandt. Excited atoms in the free-burning Ar arc: treatment of the resonance radiation. *Journal of Physics D: Applied Physics*, 49(47):475202, 2016. doi:10.1088/0022-3727/49/47/475202.

[7] J.E. Lawler, G.J. Parker, and W.N.G. Hitchon. Radiation trapping simulations using the propagator function method. *Journal of Quantitative Spectroscopy and Radiative Transfer*, 49(6):627–638, 1993. doi:10.1016/0022-4073(93)90006-4.

[8] D. Morris and K. Salisbury. Automatic preparation, calibration, and simulation of deformable objects. *Computer methods in biomechanics and biomedical engineering*, 11(3):263–279, 2008. doi:10.1080/10255840701769606.

[9] Yu.B. Golubovskii, A. Timofeev, S. Gorchakov, D. Loffhagen, and D. Uhrlandt. Population of resonance and metastable atoms in a cylindrical volume of finite size. *Physical Review E - Statistical, Nonlinear, and Soft Matter Physics*, 79(3):25–27, 2009. doi:10.1103/PhysRevE.79.036409.